Appl. Phys. A 80, 861–864 (2005)
DOI: 10.1007/s00339-003-2328-9

Applied Physics A
Materials Science & Processing

H.B. LIAO[1,2]
W. WEN[1,✉]
G.K.L. WONG[1]

Preparation and characterization of Au/SiO_2 multilayer composite films with nonspherical Au particles

[1] Department of Physics, Hong Kong University of Science and Technology, Clear Water Bay, Kowloon, Hong Kong, P.R. China
[2] Department of Physics, Beijing Normal University, Beijing, 100875, P.R. China

Received: 20 February 2003/Accepted: 25 July 2003
Published online: 1 October 2003 •

ABSTRACT Au/SiO_2 multilayer composite films containing nonspherical Au particles were prepared by a magnetron sputtering method. Uniform size and shape distributions of Au particles were obtained in these films. Au particles embedded in these films can be shaped into spheres or ellipsoids by controlling the thickness of the Au layer, and the thermal annealing temperature and time duration. Their linear optical properties were characterized in the wavelength range between 300–1000 nm. Their effective nonlinear optical susceptibility, $\chi^{(3)}$, was found to be much larger than that prepared by the cosputtering method at low Au volume fraction. We attributed the enhancement of the value of $\chi^{(3)}$ to the more uniform size and shape distribution, as well as the higher two-dimensional metal particle density in the multilayer films.

PACS 81.15.Cd, 78.66.Sq, 42.65.An

1 Introduction

Glasses doped with metal clusters, such as Au, Ag, and Cu, have been utilized widely as ornaments for almost a hundred years due to their beautiful colors, which are now known to result from the so-called surface plasmon resonance (SPR) [1, 2]. Flytzanis and coworkers gave the first report about the nonlinearities of such composites in 1985, where the third-order nonlinear optical susceptibilities, $\chi^{(3)}$, were found to be several orders of magnitude larger than that of the pure glass [3]. Since then, metal-particle-doped dielectric composites have attracted much attention as a new kind of nonlinear material with fast response time. The enhancement of $\chi^{(3)}$ in such composites was known to stem from the enhancement of the local field near the metal particles, which was related to the metal concentration and the dielectric constant of both the metal and the matrix material. Hence, in order to further improve the nonlinearity of such composites, various techniques of sample preparation, such as ion implantation [4], sputtering [5], laser ablation [6] and sol–gel [7], have been used to incorporate more metal particles into different dielectric matrices.

✉ Fax: +86-852/2358-1652, E-mail: phwen@ust.hk

Usually, metal particles with spherical shape were randomly dispersed inside these composite materials. Au particles shaped into ellipsoids and nanorods were prepared in porous glass only by ion-implantation [8] and in nanoporous alumina membranes by electrochemical deposition [9]. Two SPR peaks were observed in these materials and the splitting of SPR peaks was attributed to the longitudinal and the transverse absorption model. However, their nonlinear optical properties have not been investigated as yet. Recent theoretical studies showed that the anisotropy of both the shape and geometric distribution of the metal particles could cause a separation of the absorption peak and the enhancement of the nonlinearity [10, 11]. This means that a large figure of merit (FOM) could be obtained for these composite films, which could be of great importance for many applications. It would therefore be useful to prepare composite materials, especially in the form of thin films, with different particle-shapes and geometric distribution, in order to gain a better understanding of the origin of the enhancement of the nonlinearity, and also to further optimize the value of $\chi^{(3)}$.

In this paper, we report a simple and reproducible way to prepare Au/SiO_2 multilayer composite thin films with ellipsoidal Au particles. The size and the shape distributions of the Au particles were characterized by transmission electron microscopy, and their effective nonlinear optical susceptibilities, $\chi^{(3)}$, were measured by a standard backward degenerate four wave mixing (DFWM) scheme at 532 nm.

2 Experiment

The Au/SiO_2 multilayer films were prepared in a three-target magnetron sputtering system (Denton SJ/24 LL). In this sputtering system, the Au (99.999%) and SiO_2 (99.99%) targets, which were two inches in diameter, were connected to two independent rf power supplies. The Au layers and SiO_2 layers could be alternately deposited onto the substrates at room temperature. Oxygen was introduced into the sputtering system to prevent the SiO_2 films suffering from oxygen deficiency. The pressure ratio of $Ar : O_2$ was set to 9 : 1. The deposition rates of Au and SiO_2 were first calibrated by separately sputtering Au and SiO_2 under the same deposition conditions. Au/SiO_2 multilayer films used in the work described by this article all had the same thickness of SiO_2 layer (about 20 nm), while the thickness of the Au layer

was varied from 1 nm to 16 nm by changing the deposition time. A heat treatment of the as-grown samples was carried out in a thermal furnace, which could sustain a maximum temperature as high as 1350 °C. The heating/cooling rate and the annealing duration could be automatically adjusted by setting the program parameters. All samples were annealed at 950 °C for 10 h.

X-ray diffraction (XRD) (model: Philips PW1830) was employed to investigate the crystallinity of the Au and SiO_2. Also, the images of the cross-sectional microstructure of selected Au/SiO_2 composite films were revealed by transmission electron microscopy (TEM) (model: Philips CM120) and their size-distributions were obtained by analyzing the individual Au particles in the TEM pictures.

The linear optical absorption spectra of the Au/SiO_2 films were measured using a UV-VIS spectrophotometer (Perkin Elmer, lambda 20) in the range 300–1000 nm with a resolution of 1 nm. The third-order nonlinear susceptibility, $\chi^{(3)}$, was measured at 532 nm using a Nd : YAG laser (Q-switched and mode-locked) and employing a standard backward degenerate four-wave mixing (DFWM) scheme. The laser had a pulse duration of 70 ps, a repeat rate of 500 Hz, and a maximum peak power of about 6.5 MW cm^{-2}. A high sensitivity photodiode and a lock-in amplifier were used to detect the nonlinear signals. The value of the effective $\chi^{(3)}$ was measured relative to CS_2 (a reference medium which had $\chi^{(3)} \cong 2 \times 10^{-12}$ esu in the picosecond time scale) via the following equation [12]:

$$\chi^{(3)} = \chi^{(3)}_{CS_2} \sqrt{\frac{I_s}{I_{CS_2}} \frac{n_s^2}{n_{CS_2}^2} \frac{L_{CS_2}}{L_s} \frac{\ln \frac{1}{T}}{(1-T)\sqrt{T}}} \quad (1)$$

where I_s and I_{CS_2} were the intensity of the conjugate signals, n_s and n_{CS_2} were the refractive indices, L_s and L_{CS_2} were the thicknesses of the Au/SiO_2 composite films and the CS_2 respectively, and T was the transmissivity of the Au/SiO_2 films at a given laser wavelength.

3 Results and discussion

The most striking changes of the Au/SiO_2 multilayer films induced by the thermal annealing are their colors. Before annealing, the colors of the films are dark brown. After annealing, their colors changed to ruby-like for the films with a thinner Au layer, or golden-like for those with a thicker Au layer due to the formation of Au particles. The crystallization of some selected composite films measured by XRD methods are displayed in Fig. 1. For the samples with an Au layer of 1 nm, the diffraction peaks of Au particles are very weak (Fig. 1a), even after annealing at 950 °C for 10 hours, due to the small Au particles and low Au concentration. However, as the thickness of the Au layer increases to 4 nm (Fig. 1b) and 8 nm (Fig. 1c), the peaks become much sharper and higher. This indicates that the Au particles have become much larger. By comparing the peak intensity of the Au(111) and Au(200), we know that the Au crystallites have a texture structure along the ⟨111⟩ direction. The broad peak around $2\theta = 22°$ is attributed to the diffraction from the quartz substrate and the SiO_2 films. Obviously, there is no crystallized SiO_2 in these annealed samples.

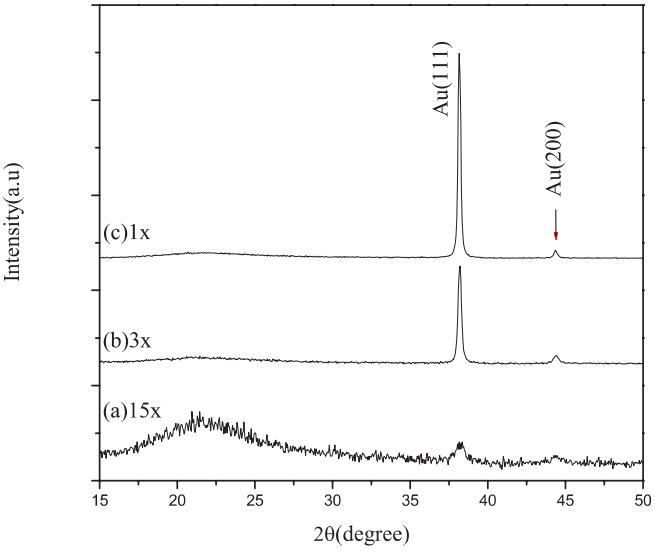

FIGURE 1 The X-ray diffraction patterns of the Au/SiO_2 multilayer films annealed at 950 °C for 10 h. The thickness of the Au layers are: **a** 1 nm; **b** 4 nm; **c** 8 nm

The cross-sectional TEM pictures of some selected samples are shown in Fig. 2. As seen from Fig. 2a, the Au particles are spherical in the film with an Au layer thickness of 1 nm. Although its multilayer structure is not very clear, the distance between the Au particles in the direction parallel to the film surface is found to be smaller than that perpendicular to it due to the island-like growth model of the very thin Au layer. This morphology is very similar to that reported in reference [13]. However, under the same annealing conditions, with increasing thickness of the Au layer, the Au particles become ellipsoid at a thickness of 4 nm (Fig. 2b) and 8 nm (Fig. 2c) respectively, and then they become pancake-like (Fig. 2d) with further increasing thickness to 16 nm. Multilayer structures can be clearly observed in these annealed samples.

Here we define the aspect ratio of the Au particle as a/z, where a is the dimension parallel to the film surface and z is the one perpendicular to it. Also, we name the particle as ellipsoid if the aspect ratio is in the range of 1–2, and pancake-like if more than 2. According to this definition, we find that ellipsoidal Au particles can be formed in Au layers of thickness of 3–12 nm. Au particles are spherical for the thinner layers or pancake-like for thicker layers. The size of the ellip-

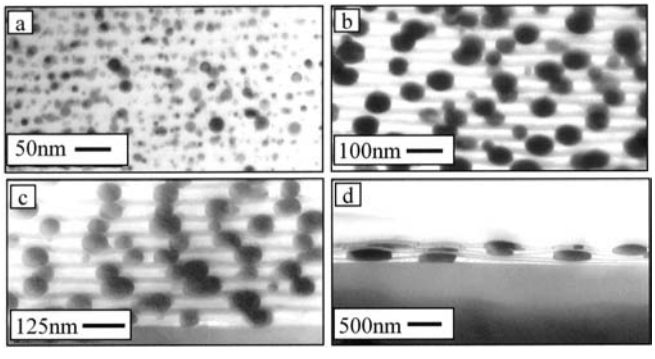

FIGURE 2 Selected cross-sectional TEM pictures of the Au/SiO_2 multilayer films annealed at 950 °C for 10 h. The thickness of the Au layers are: **a** 1 nm; **b** 4 nm; **c** 8 nm; **d** 16 nm

soidal Au particles (the dimension of a) can be changed in the range of 20–150 nm by varying the thickness of the Au layer, and the annealing temperature and time duration. A suitable annealing temperature and an amorphous dielectric layer are very important for maintaining the multilayer structure and for forming ellipsoid Au particles. For example, we found that, when annealed at 1050 °C for 5 h, the SiO_2 layers became soft and then connected with each other. In this situation, Au from different layers passed through the SiO_2 layers and coalesced to form very large spherical particles. On the other hand, when replacing half of the SiO_2 layers by TiO_2 ones, we noticed that a similar phenomenon occurred due to the cystallization of TiO_2 after thermal annealing, although the film had a well defined multilayer structure before annealing. A layer thickness of SiO_2 of more than 10 nm is also necessary to form continuous films and to guarantee a multilayer morphology.

The TEM images suggest that our samples have a fairly uniform distribution both in particle shape and size. A micrograph field including more than 200–250 particles was randomly selected to analyze the size distribution of the Au particles. The typical size distributions of the samples are plotted in Fig. 3. The spherical Au particles in the film used in Fig. 2a (see curve a in Fig. 3) have a mean size of 9.5 nm with a deviation of 21%. For the sample used in Fig. 2c, we give two statistical size-distributions: one is perpendicular to the film surface (curve b in Fig. 3) and the other is parallel to it (curve b′ in Fig. 3). Their standard deviation, derived using a Gaussian curve fit, is about 18.5% and 20% respectively. The film used in Fig. 2b has a similar size distribution to that used in Fig. 2c. This result reveals that a $SiO_2/Au/SiO_2$ sandwich-like structure can really confine the growth of the Au particles and give a uniform size and shape distribution.

The UV-VIS spectra are shown in Fig. 4, which are normalized to an Au film with total thickness of 40 nm. As seen from Fig. 4, with increasing thickness of the Au layer from 1 nm to 8 nm (see Fig. 4a–c), the SPR peaks shift from 528 nm

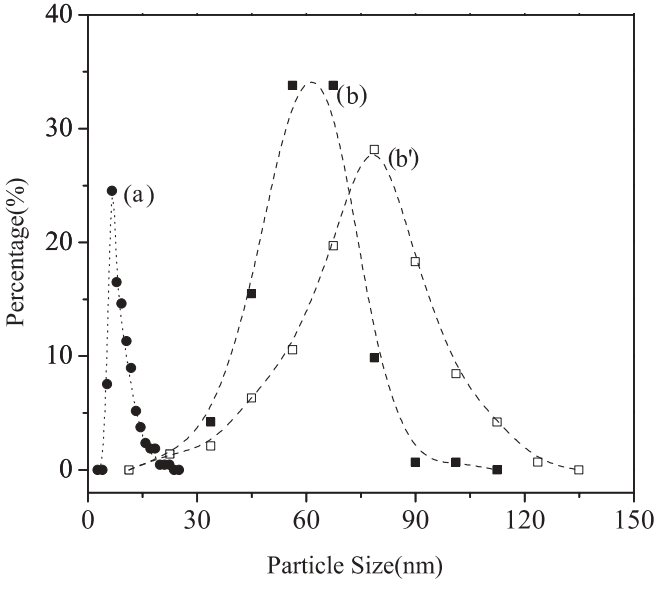

FIGURE 3 The statistical size-distributions of the Au particles: **a** for the film shown in Fig. 2a; **b** perpendicular to the film surface for the film used in Fig. 2c; **b'** parallel to the film surface for the film used in Fig. 2c

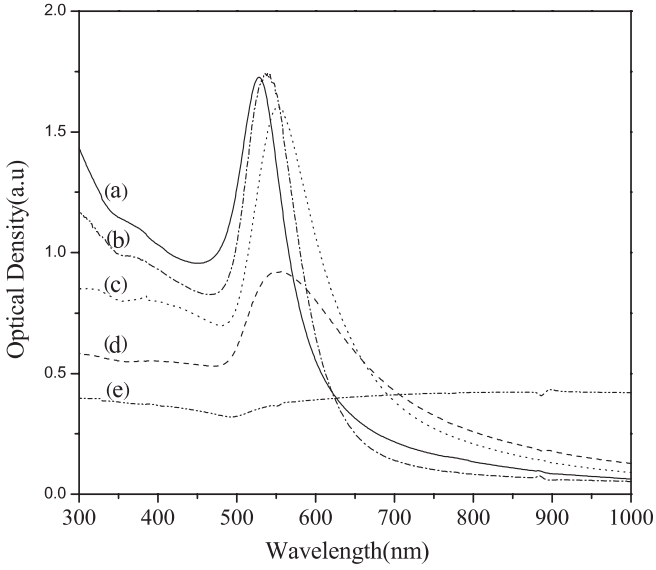

FIGURE 4 The UV-VIS spectra of the Au/SiO_2 multilayer films, which were normalized to a total Au thickness of 40 nm. The thicknesses of the Au layers are: **a** 1 nm; **b** 4 nm; **c** 8 nm; **d** 12 nm; **e** 16 nm

to 553 nm. The redshift observed in Fig. 4 should be attributed to two aspects: increasing particle size and ellipsoidal-shape formation. Here, we have not observed a splitting of the SPR peak as reported in some references [9, 14], probably because the aspect ratios of our ellipsoidal Au particles are not large enough (only about 1.2–1.5). Hence, the peak of the longitudinal plasmon, which is usually in the longer wavelength range, is very close to that of the transverse one. As a result, these two peaks are indistinguishable and then it only causes a redshift of the surface plasmon. However, for the sample with an Au layer of 11 nm (Fig. 4d), the intensity of the SPR peak decreases, while the SPR peak smears out. The film has a very weak optical density in the range of 300 nm to 1000 nm when the Au layer reaches the thickness of 16 nm (Fig. 4c) due to the broadening of the SPR peak and the intense light scattering caused by the very large particles (more than 100 nm).

The effective third-order nonlinear susceptibilities, $\chi^{(3)}$, are listed in Table 1, where the volume fraction of Au is estimated by the growth rate and the deposition time of the Au and SiO_2 components ($Au/(Au + SiO_2)$), and the mean size is obtained by analyzing the TEM pictures. As listed in Table 1, the $\chi^{(3)}$ of the Au/SiO_2 with a thin Au layer of about 1 nm is only 1×10^{-7} esu and its figure of merit (FOM), $\chi^{(3)}/\alpha$,

Sample	Thickness of Au layer (nm)	Volume fraction of Au (%)	Mean size of Au particle (nm)	$\chi^{(3)}$ (esu)	$\chi^{(3)}/\alpha$ (esu)
1	1	4.5	9.5	1×10^{-7}	2.1×10^{-12}
2	2	8.7	23.5	6.0×10^{-7}	7×10^{-12}
3	4	16	50×61	2.4×10^{-6}	2.5×10^{-11}
4	8	26.7	60×75	2.1×10^{-6}	2.55×10^{-11}
5	12	35	92×134	—	—
6	16	40	160×530	—	—

TABLE 1 The third order nonlinear susceptibilities, $\chi^{(3)}$, and the figure of merit, $\chi^{(3)}/\alpha$, of the Au/SiO_2 multilayer films

is about 2.1×10^{-12} esu, where α is the absorption coefficient of the composite film at the laser wavelength. But with increasing Au thickness (the thickness of SiO_2 remains the same) to 2 nm and 4 nm, the $\chi^{(3)}$ increases to 6×10^{-7} esu and 2.4×10^{-6} esu, and the FOM increases to 7×10^{-12} esu and 2.5×10^{-11} esu, respectively. When further increasing the Au layer to 8 nm, the value of $\chi^{(3)}$ and the FOM (about 2.1×10^{-6} esu and 2.55×10^{-11} esu, respectively) changes a little with respect to that of the film having a 4 nm Au layer. The $\chi^{(3)}$ of the films with Au layers of 12 nm and 16 nm are almost immeasurable due to the intense light scattering caused by the very large Au particles (as seen in Table 1).

Obviously, the values of both $\chi^{(3)}$ and FOM increase nonlinearly with increasing Au volume fraction. A similar relationship between the $\chi^{(3)}$ and the Au concentration has been reported in reference [5]. But the value of $\chi^{(3)}$ measured for our lower Au volume fraction multilayer films was about two orders greater than those prepared by the co-sputtering method, although they were all prepared in the same sputtering system and we used the same method to estimate the volume fraction. Also, their nonlinearities were measured using the same laser. However, the multilayer films have a value of $\chi^{(3)}$ as large as 2.5×10^{-6} esu at a volume fraction of 16%, while the co-sputtering films reach that value at 40%. Therefore, we suppose that although the total volume fraction of Au is the same, multilayer films may have a larger two-dimensional particle density than that of co-sputtering films. In other words, the interaction between the Au particles should play an important role for the enhancement of the nonlinearities of such metal-dielectric composites. Of course, the more uniform size and shape distribution of the Au particles in the multilayer films may also be attributed to the enhancement of $\chi^{(3)}$ because we have found that the $\chi^{(3)}$ may reach a maximum value for Au particle size of around 30 nm [15].

4 Conclusions

We prepared Au/SiO_2 multilayer composite thin films with nonspherical Au particles using a magnetron sputtering system. A uniform particle size and shape distribution was obtained for these films. It was found that their $SiO_2/Au/SiO_2$ sandwich-like structure can slow down the growth of the Au particles in a particular direction, resulting in an anisotropy of the shape of Au particles. Au particles embedded in these films can be made to be spherical or ellipsoidal in shape by controlling the thickness of Au layer, and the thermal annealing temperature and time duration. Their linear optical properties were characterized over the wavelength range of 300–1000 nm. Their effective nonlinear optical susceptibilities, $\chi^{(3)}$, were found to be larger than those of films prepared via the co-sputtering method. We attributed the enhancement of the value of $\chi^{(3)}$ to the more uniform size and shape distribution, as well as the higher two-dimensional particle density in the multilayer films.

ACKNOWLEDGEMENTS This work was supported by RGC Hong Kong through Grants No. N_HKUST025/00 and No. HKUST6153/00P.

REFERENCES

1 C. Flytzanis, F. Hache, M.C. Klein, D. Ricard, P. Rousignol: In *Progress in Optics XXIX*, ed. by E. Wolf (Elsevier, Amsterdam, 1991), p321.
2 U. Kreibig, M. Vollmer: *Optical Properties of the Metal Clusters* (Springer-Verlag, Berlin, Heidelberg, 1995)
3 D. Ricard, P. Roussignol, C. Flytzanis: Opt. Lett. **10**, 511 (1985)
4 R.H. Magruder III, L. Yang, R.F. Haglund, C.W. White, L. Yang, R. Dorsinville, R.R. Alfano: Appl. Phys. Lett. **62**, 1730 (1993)
5 H.B. Liao, R.F. Xiao, J.S. Fu, P. Yu, G.K.L. Wong, P. Sheng: Appl. Phys. Lett. **70**, 1 (1997)
6 J.M. Ballesteros, R. Serna, J. Solis, C.N. Afonso, A.K. Pertford-Long, D.H. Osborne, R.F. Haglund, Jr.: Appl. Phys. Lett. **71**(17), 2445 (1997).
7 T. Ishizaka, S. Muto, Y. Kurokawa: Opt. Commun. **190**, 385 (2001)
8 D.O. Henderson, A. Ueda, R. Mu, Y.S. Tung, M. Wu, J. Chen, Z. Gu, C.W. White, R. Zuhr, J.G. Zhu, L. Xi: Proceedings of the fourth International Symposium on Quantum confinement: Nanoscale Materials, Devices and Systems, Montreal, Que., Canada. 4–7 May 1997
9 G.L. Hornyak, C.R. Martin: Thin Solid Film **303**, 84 (1997)
10 K.P. Yuen, M.F. Law, K.W. Yu, P. Sheng: Phys. Rev. E **56**(2), R1322 (1997)
11 L. Gao, K.W. Yu, Z.Y. Li, B. Hu: Phys. Rev. E **64**, Number 036615 (2001)
12 R.L. Sutherland (Ed.): *Handbook of Nonlinear Optics* (Marcel Dekker, Inc. New York, 1996)
13 I. Tanahashi, Y. Manabe, T. Tohda, S. Sasaki, A. Nakamura: J. Appl. Phys. **79**, 1224 (1996)
14 S. Link, M.A. El-Sayed: J. Phys. Chem. B **103**(40), 8410 (1999)
15 H.B. Liao, W. Wen, G.K.L. Wong: J. Appl. Phys. **93**(8), 4485 (2003)